Chemical Engineering Science 271 (2023) 118524

Contents lists available at ScienceDirect

Chemical Engineering Science

journal homepage: www.elsevier.com/locate/ces

A novel method for the globally optimal design of fixed bed catalytic reactors

André L.M. Nahes [a], Miguel J. Bagajewicz [b,c], André L.H. Costa [a,*]

[a] Institute of Chemistry, Rio de Janeiro State University (UERJ), Rua São Francisco Xavier, 524, Maracanã, Rio de Janeiro, RJ CEP 20550-900, Brazil
[b] School of Chemical, Biological and Materials Engineering, University of Oklahoma, Norman Oklahoma 73019, United States
[c] Federal University of Rio de Janeiro (UFRJ), Escola de Química CT, Bloco E, Ilha do Fundão, CEP 21949-900 Rio de Janeiro, RJ, Brazil

HIGHLIGHTS

- A new procedure for the optimal design of fixed bed reactor is proposed.
- The reactor investigated is composed of a tube bundle with catalyst inside a shell.
- Optimization method employed: Partial Set Trimming followed by Smart Enumeration.
- The method always attain the global optimum without convergence drawbacks.
- Proposed method presents a better performance than two different metaheuristics.

ARTICLE INFO

Article history:
Received 7 October 2022
Received in revised form 21 December 2022
Accepted 24 January 2023
Available online 1 February 2023

Keywords:
Fixed Bed Reactors
Design
Optimization
Set Trimming
Enumeration

ABSTRACT

Fixed bed reactors are usually designed using simulation approaches by trying different dimensions as well as operating conditions followed by verification if the desired conversion is achieved. This trial and verification procedure does not guarantee optimality, just a feasible and reasonably good design (depending on the expertise of the designer). Cost minimization or profit maximization using optimization procedures is more rigorous, but it has been rarely employed. The methods usually employed in the literature for solving this design problem present limitations. In this article, we solve the design problem of fixed bed catalytic reactors globally. We use Partial Set Trimming followed by Smart Enumeration, a recently developed rigorous global optimization procedure. The reactor investigated is composed of a tube bundle, filled with a catalyst, inside a shell containing boiling water. We compare the performance of the proposed approach with the use of metaheuristics-based tools, which do not guarantee optimality.

1. Introduction

Fixed bed catalytic reactors abound in chemical process industries. They are essential in the production of several chemical commodities, such as methanol, ammonia, ethylene oxide, styrene, cyclohexane, etc. (Hagen, 2015).

Given their importance, their simulation has been the object of many studies. The simulation of fixed bed reactors involves the solution of mass, energy, and momentum balances, associated with a given kinetic rate expression of each reaction, as reviewed by Froment and Bischoff (1990), covering one-dimensional and two-dimensional models, pseudo-homogeneous and heterogeneous models, as well as plug flow and nonideal flow models.

While the aforementioned simulation works were useful for the assessment of the reactors performance, the problem of obtaining the best design, that is, the best geometry and operational variables for a given cost or profit objective, abiding by design constraints (minimum conversion, pressure drop limitations, limitations on side products, maximum temperature, slenderness, etc.) have emerged as an important need.

Different objective functions, such as minimization of annualized capital and operational costs (Zhou and Manousiouthakis, 2008) and maximization of the product revenue (Vakili and Eslamloueyan, 2013) have been used. Despite the several alternatives for reactor modeling mentioned above, previous works about reactor design optimization were based on unidimensional pseudo-homogeneous models. These mathematical models are based on differential equations of mass, energy, and eventually, momentum balances when pressure drop is of importance. These equations may be discretized in a set of algebraic equations, to

* Corresponding author.
E-mail address: andrehc@uerj.br (A.L.H. Costa).

https://doi.org/10.1016/j.ces.2023.118524
0009-2509/

Nomenclature

$\widehat{\boldsymbol{a}}$	Catalyst activity
A_c	Tube reactor cross-section area (m^2)
$\widehat{a}_v$	Specific surface area of catalyst bed (m^2/m^3)
b_k	Effectiveness factor model parameter
C_i	Concentration of component i (kmol/m^3)
C_i^s	Concentration of component i in the solid phase (kmol/m^3)
$CAPEX$	Capital cost ($)
$\widehat{CL}$	Geometrical constant
Cpm	Mixture heat capacity (J/(kg·K))
dte	Outer diameter (m)
$\widehat{dti}$	Inner diameter (m)
$\widehat{D}_p$	Catalyst particle diameter (m)
Dsi	Inner diameter of the shell (m)
$\widehat{E}$	Joint efficiency
F_i	Molar flow rate of component i (kmol/s)
$\widehat{F}_{product}^{min}$	Minimum production of the key prodcut (kmol/s)
f_t^{NPV}	Present value factor
G	Mass flux (kg/(s·m^2))
ht	Convective heat transfer coefficient of the gas phase (W/(m^2·K))
hs	Convective heat transfer coefficient of the boiling water (W/(m^2·K))
h_f	Fluid-solid heat transfer coefficient (W/(m^2·K))
$\widehat{i}$	Interest rate
$\widehat{k}_{tube}$	Tube wall thermal conductivity (W/(m·K))
k	Constant for the reverse ammonia reaction
$k_{i,j}$	Binary coefficient of Equation of State
k_{gi}	Mass transfer coefficient for component i (m/s)
Ka	Equilibrium constant
L	Tube length (m)
NPC	Net Present Cost ($)
Ltp	Tube pich (m)
Ntt	Total number of tubes
$\widehat{N}_{cat}$	Number of catalyst loadings
$OPEX$	Present value of cost of the catalyst ($)
P	Pressure (Pa)
Pd	Maximum vessel pressure difference (Psi)
$\widehat{p}_{cat}$	Catalyst price ($/kg)
$\widehat{p}_{mat}$	Reactor material price ($/kg)
r_j	Reaction rate of reaction j (kmol/(s·kg catalyst))
$r_{product}^{UB}$	Maximum reaction rate (kmol/(s·kg catalyst))
$\widehat{S}$	Allowable tensile strength (psi)
$\widehat{\boldsymbol{n}}_{\boldsymbol{t}}$	Time of the catalyst change (y)
T	Gas temperature (K)
$\boldsymbol{T}^{\boldsymbol{s}}$	Solid temperature (K)
$\widehat{\boldsymbol{T}}_{\boldsymbol{max}}$	Maximum temperature (K)
Tc	Boiling water temperature (K)
Tin	Inlet temperature (K)
thk_{head}	Head thickness (m)
thk_{shell}	Shell thickness (m)
$thk_{tubesheet}$	Tubesheet thickness (m)
U	Overall heat transfer coefficient (W/(m^2·K))
V_{cat}	Reactor catalyst volume (m^3)
W_{cat}	Catalyst mass (kg)
W_{req}^{LB}	Lower bound of the required catalyst mass (kg)
$W_{reactor}$	Reactor mass (kg)
W_{tubes}	Tube mass (kg)
W_{shell}	Shell mass (kg)
$W_{tubesheet}$	Tubesheet mass (kg)
W_{heads}	Head mass (kg)
X_i	Conversion of component i
z	Spatial coordinate (m)

Greek Symbols

$\widehat{\upsilon}_{ij}$	Stoichiometric coefficient of component i in reaction j
$\widehat{\eta}_j$	Catalyst effectiveness of reaction j
$\widehat{\rho}_B$	Bed density (kg/m^3)
$\widehat{\rho}_{mat}$	Density of the reactor material (kg/m^3)
ρ	Fluid density (kg/m^3)
$(\Delta H_r)_j$	Enthalpy of reaction j (J/(kmol))
ΔP	Total pressure drop (bar)
ΔP^{LB}	Lower bound on the pressure drop (bar)
$\Delta\widehat{Pdisp}$	Available pressure drop (bar)
$\left(\frac{\Delta P}{\Delta z}\right)^{LB}$	Lower bound of the pressure gradient (Pa/m)
$\widehat{\phi}$	Bed void fraction
μ	Fluid viscosity (Pa·s)

which some inequalities related to slenderness, maximum temperatures, maximum pressure drop, etc., are added. Aside from trial and verification using simulation, two classes of optimization approaches were employed: mathematical programming and metaheuristic algorithms. We discuss these methods in detail later.

We concentrate on reviewing methods used for the optimal design of ammonia and methanol reactors, which are germane to our results section. Several authors investigated the design optimization of ammonia synthesis reactors considering the maximization of the profit, using the formulation presented by Murase et al. (1970). Edgar et al. (1989) solved this problem using the Generalized Reduced Gradient method, employing the solver GRG2. The evaluation of the constraints was conducted using the solver LSODE for the numerical solution of the set of differential equations. Yancy-Caballero et al. (2015) addressed this problem using a mathematical programming approach by discretizing the differential equations involved. The resultant nonlinear programming (NLP) problem was solved using the IPOPT solver (Wächter and Biegler, 2006). Carvalho et al. (2014) and Matos et al. (2021) solved this design problem based on unconstrained formulations, using the barrier method (by inserting the constraints into the objective function with a penalty). Some authors used *meta*-heuristic/stochastic methods: Genetic Algorithms (GA) (Upreti and Deb, 1997; Babu and Angira, 2005) and Differential Evolution (DE) (Angira, 2011).

In turn, the optimization of methanol synthesis reactors was investigated using different objective functions. The minimization of the catalyst volume in the design of spherical methanol reactors was investigated by Hartig and Keil (1993). They employed Iterative Dynamic Programming (IDP), Sequential Quadratic Programming (SQP), and the Complex method, associated with the solution of the differential equations using the Runge-Kutta method. Grue and Bendtsen (2003) addressed the entire synthesis loop and employed a reactor mathematical model discretized using orthogonal collocation points on finite elements. The resultant problem with constraints represented by algebraic equations was solved using an undisclosed NLP solver through the GAMS interface. Genetic Algorithms were used by Torcida et al. (2022) to maximize profit, considering the annualized costs of equipment.

All the aforementioned techniques present limitations. Metaheuristic algorithms depend on parameter tuning and do not guarantee global optimality. They often give good solutions when compared to the global optimum obtained by other means, a condition that the user cannot know unless he/she tries both methods.

Mathematical programming many times presents convergence problems and computational time limitations. In addition, local solvers sometimes end up trapped in local minima.

This article departs from the above-described approaches and addresses the problem using Partial Set Trimming followed by Smart Enumeration, a recently developed technique formalized by Costa and Bagajewicz (2019), originally presented by Gut and Pinto (2004) applied to a very particular case. This solution procedure can identify the global optimum solution without using any gradient-based search and/or branch and bound procedure typical of mathematical programming. Contrasting with the set of variables typically used in mathematical programming for the solution of design problems, mixing discrete and continuous variables; in our technique, the search space is described by a combinatorial representation of discrete variables, where each solution candidate is represented by a set of values of the discrete variables. Set Trimming explores inequality constraints to reduce the number of solution candidates. Additionally, we introduce Proxy Set Trimming, which is based on upper and lower bounds associated with more complex constraints for generating simpler mathematical relations for candidate set elimination. Smart Enumeration consists of organizing the candidates in increasing order of a lower bound of their objective function and evaluating them one by one until one obtains a feasible candidate, which becomes an incumbent. After that, the evaluation continues (updating the incumbent when a candidate is feasible and has a lower value of the objective function) and stops when the lower bound is larger than the incumbent objective function (Costa and Bagajewicz, 2019). More details are given in a specific section later in the article.

2. Reactor mathematical model

There are different alternatives of fixed-bed reactors, such as adiabatic reactors, quasi-isothermal reactors, quench reactors, etc. (Moulijn et al., 2013). Without loss of generality, we apply our proposed optimization approach to a reactor composed of a tube bundle filled with the catalyst inside a shell. The reaction is exothermic and the shell contains boiling water. Fig. 1 depicts a representation of the reactor structure.

There are two broad categories in fixed-bed reactor modeling: pseudo-homogenous and heterogeneous models (Froment and Bischoff, 1990). The difference between them is the strategy to deal with the solid phase, where the first does not account for it explicitly, and the second one considers mass and energy balance equations for the fluid and solid phases. According to the literature review performed above, the papers that addressed the design optimization problem of fixed-bed reactors were based on pseudo-homogeneous models.

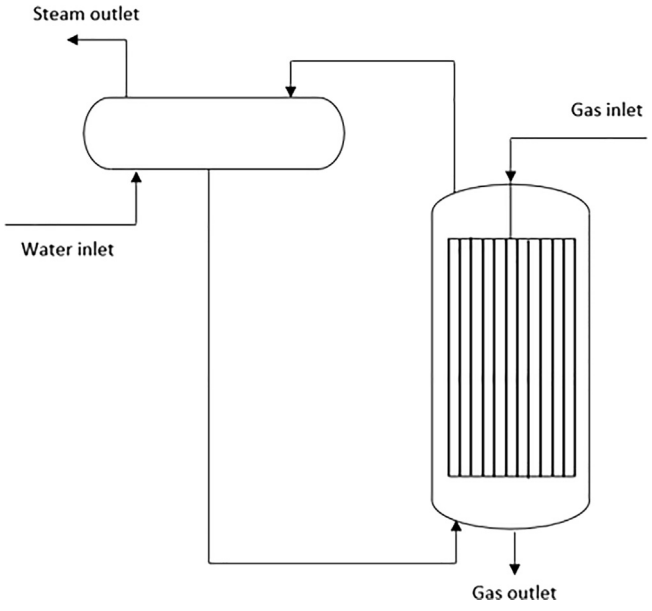

Fig. 1. Fixed-bed reactor.

It is important to observe that our design-optimization approach for the design of fixed-bed reactors is flexible and can be applied to any kind of model. In the current paper, we use both models to illustrate this aspect of our methodology, without the intention of discussing the validity and accuracy of each model.

2.1. Pseudohomogenous model

We use a steady-state one-dimensional pseudo-homogeneous plug flow model (Santangelo et al., 2008). The molar balance in a single reactor tube is given by (the model parameters are represented with a symbol ^ on top):

$$\frac{dF_i}{dz} - \sum_j \left(\hat{\upsilon}_{ij} r_j\right) \hat{a}\, \hat{\eta}_j\, \hat{\rho}_B\, A_c = 0 \tag{1}$$

where F_i is the molar flow rate of component i in a single tube, z is the spatial coordinate, $\hat{\upsilon}_{ij}$ is the stoichiometric coefficient of component i in reaction j, r_j is the rate of reaction j, $\hat{a}$ is the catalyst activity, $\hat{\eta}_j$is the catalyst effectiveness of reaction j (assumed constant), $\hat{\rho}_B$ is the bed density and A_c is the tube reactor cross-section area associated with an inner diameter dti. The cross-sectional area is:

$$A_c = \pi \frac{dti^2}{4} \tag{2}$$

In turn, the energy balance is given by:

$$GCp_m \frac{dT}{dz} - \sum_j \left(-\left(\widehat{\Delta H_r}\right)_j r_j\right) \hat{a}\, \hat{\eta}_j\, \hat{\rho}_B - U \frac{\pi dte}{A_c} (T - Tc) = 0 \tag{3}$$

where G is the mass flux, Cp_m is the mixture heat capacity, $\left(\widehat{\Delta H_r}\right)_j$ is the enthalpy of reaction j. Temperatures T and Tc correspond to the fluid and the boiling water (cold utility), respectively, and U is the overall heat transfer coefficient. Ignoring fouling, the expression of the overall heat transfer coefficient becomes:

$$U = \frac{1}{\frac{1}{ht}\left(\frac{dte}{dti}\right) + \frac{dte\, ln\left(\frac{dte}{dti}\right)}{2\hat{k}_{tube}} + \frac{1}{hs}} \tag{4}$$

where dti and dte are the inner and outer tube diameters, $\hat{k}_{tube}$ is the tube wall thermal conductivity, ht and hs are the convective heat transfer coefficients of the gas phase flowing inside the tubes and of the boiling water in the shell.

The momentum balance is given by the Ergun equation (Ergun, 1952):

$$\frac{dP}{dz} = -\frac{G}{\rho \hat{D}_p}\left(\frac{1-\hat{\phi}}{\hat{\phi}^3}\right)\left[\frac{150\left(1-\hat{\phi}\right)\mu}{\hat{D}_p} + 1.75G\right] \tag{5}$$

where P is the pressure, $\hat{D}_p$ is the catalyst particle diameter, $\hat{\phi}$ is the bed void fraction, and ρ and μ are the fluid density and viscosity.

In addition, the reactor is full of boiling water; therefore, a two-phase saturated stream leaves the reactor. Finally, the diameter of the shell is calculated as a function of the number of tubes, their diameter, the pitch ratio, and the tube layout (see Kakaç and Liu, 2002). Without loss of generality, the pitch ratio and layout are considered fixed.

2.2. Heterogeneous model

The heterogeneous model used in this paper also assumes a steady-state plug flow pattern and considers the intraparticle concentration gradient through an effectiveness factor.

The mass and energy balances for the fluid phase and the solid phase are given by:

$$\frac{dF_i}{dz} = A_c\, k_{gi}\, \hat{a}_v (C_i^s - C_i) \tag{6}$$

$$GCp_m \frac{dT}{dz} = h_f \hat{a}_v (T^s - T) + \pi \frac{dte}{Ac} U(Tc - T) \tag{7}$$

$$-\sum_j (\hat{\upsilon}_{ij}\, r_j\, \hat{a}\, \hat{\eta}_j)\rho_B = k_{gi}\, \hat{a}_v (C_i - C_i^s) \tag{8}$$

$$-\sum_j \left(\widehat{\Delta H_r}\right)_j \hat{\rho}_B r_j \hat{a}\, \hat{\eta}_j = h_f \hat{a}_v (T^s - T) \tag{9}$$

where $\hat{a}_v$ is the specific surface area of the catalyst bed, k_{gi} is the mass transfer coefficient for component i, h_f is the heat transfer coefficient between the solid and fluid phases, C_i is the concentration of component i and the superscript s refers to the solid phase. The momentum balance is also given by Eq. (5).

The mass transfer coefficient is evaluated by the following expression (Cussler, 1984):

$$\frac{k_{gi}}{v^0} = 1.17 \left(\frac{\hat{D}_p v^0 \rho}{\mu}\right)^{-0.42} \left(\frac{D_{im}\rho}{\mu}\right)^{2/3} \tag{10}$$

where v^0 is the superficial velocity and D_{im} is the diffusion coefficient of component i in the fluid mixture. The diffusion coefficients depend on the molar fractions (y_i) and the binary diffusion coefficients (D_{ij}) (Fairbanks and Wilke, 1950):

$$D_{im} = \frac{1 - y_i}{\sum_{j \neq i} \frac{y_j}{D_{ij}}} \tag{11}$$

The binary diffusion coefficients can be calculated by (Reid et al., 1997):

$$D_{ij} = \frac{0.00143 T^{1.75}}{P \hat{M}_{ij}^{1/2} \left[\left(\sum \hat{v}\right)_i^{\frac{1}{3}} + \left(\sum \hat{v}\right)_j^{\frac{1}{3}}\right]^2} \tag{12}$$

where $\sum \hat{v}$ is the summing of atomic diffusion volumes. The parameter M_{ij} is given by:

$$\hat{M}_{ij} = 2\left[\frac{1}{\hat{M}_i} + \frac{1}{\hat{M}_j}\right]^{-1} \tag{13}$$

where $\hat{M}_i$ and $\hat{M}_j$ are the molar mass of the components i and j. Finally, the heat transfer coefficient between the gas and solid phases is obtained by the following correlation (Smith, 1980):

$$\frac{h_f}{Cp_m G} Pr^{2/3} = \frac{0.458}{\hat{\phi}} \left(\frac{\hat{D}_p v^0 \rho}{\mu}\right)^{-0.407} \tag{14}$$

where Pr is the Prandl number.

3. Design optimization

The optimization problem consists of the design of a reactor that attains a given minimum production according to a previously established mass and energy balance of the reaction unit, frequently associated with a recycle and a purge.

The optimization variables for the reactor design are (the reactor is considered to operate assuming a given inlet temperature and pressure of the feed stream):

- Total number of tubes (Ntt),
- Tubes inner and outer diameter (dti and dte),
- Tube length (L),
- Boiling water temperature (Tc).

Because of its physical nature or commercial availability, the geometric variables are discrete. The boiling water temperature is a continuous variable, but because Set Trimming requires discrete variables, we also use a set of discrete temperature values.

The objective function we use is the Net Present Cost (NPC), composed of the capital cost associated with the reactor construction ($CAPEX$) and the present value of the cost of the catalyst loadings during the project life ($OPEX$):

$$NPC = CAPEX + OPEX \tag{15}$$

The $OPEX$ is given by:

$$OPEX = \sum_{t=1}^{\widehat{N}_{cat}} \widehat{f}_t^{NPV}\, \hat{p}_{cat}\, \hat{\rho}_B V_{cat} \tag{16}$$

where $\hat{p}_{cat}$ is the catalyst price per unit mass, V_{cat} is the reactor catalyst volume, $\widehat{f}_t^{NPV}$ is the present value factor associated with the catalyst loading t ($t = 1, 2, \cdots, \widehat{N}_{cat}$) and $\widehat{N}_{cat}$ is the number of catalyst loadings during the horizon time of the project, which, without loss of generality, is considered fixed. In turn, the present value factor is given by:

$$\widehat{f}_t^{NPV} = \frac{1}{\left(1 + \widehat{i}\right)^{\widehat{n}_t}} \tag{17}$$

where $\widehat{n}_t$ is the number of years for the insertion of the catalyst loading t and $\widehat{i}$ is the corresponding interest rate. The frequency of catalyst loadings is given. Finally, the reactor catalyst volume is given by:

$$V_{cat} = Ntt\, \pi \frac{dti^2}{4} \tag{18}$$

On the other hand, the capital cost is estimated based on the material cost to build the reactor:

$$CAPEX = \hat{p}_{mat} W_{reactor} \tag{19}$$

where $\hat{p}_{mat}$ is the unit price of the reactor material and $W_{reactor}$ is the reactor mass. The reactor mass is composed of the mass of the tubes (W_{tubes}), shell (W_{shell}), tubesheet ($W_{tubesheet}$), and shell heads (W_{heads}):

$$W_{reactor} = W_{tubes} + W_{shell} + W_{tubesheet} + W_{heads} \tag{20}$$

$$W_{tubes} = \hat{\rho}_{mat} Ntt \frac{\pi}{4} \left(dte^2 - dti^2\right) L \tag{21}$$

$$W_{shell} = \hat{\rho}_{mat} \frac{\pi}{4} \left(\left(Dsi + 2thk_{shell}\right)^2 - Dsi^2\right) L \tag{22}$$

$$W_{tubesheet} = \hat{\rho}_{mat} \pi \frac{Dsi^2}{4} thk_{tubesheet} \tag{23}$$

$$W_{head} = \hat{\rho}_{mat} \frac{\pi}{6} \left(\left(Dsi + 2thk_{head}\right)^3 - Dsi^3\right) \tag{24}$$

where $\hat{\rho}_{mat}$ is the density of the reactor material, Dsi is the inner diameter of the shell, thk_{shell} is the shell thickness, $thk_{tubesheet}$ is the

tubesheet thickness, thk_{head} is the cover thickness. The expression of the mass of the shell heads is associated with a hemispherical alternative. The set of available inlet and outlet tube diameters corresponds to the standard values, considering a minimum wall thickness evaluated by (Fischer et al., 2020):

$$thk_{tube} = \max\left(\frac{\widehat{Pd}(dti/2)}{\widehat{S}\widehat{E} - 0.6Pd}, \widehat{thk}_{min}\right) \tag{25}$$

where $\widehat{Pd}$ is the maximum vessel pressure difference, $\widehat{S}$ is the allowable tensile strength, $\widehat{E}$ is the joint efficiency, and $\widehat{thk}_{min}$ is a minimum thickness value. The maximum pressure difference is the difference between the design pressure and the atmospheric pressure (i.e. a shell depressurization scenario). The design pressure corresponds to the feed inlet pressure multiplied by a safety factor.

Based on geometrical relations employed for shell and tube heat exchanger design, the inner shell diameter needed to accommodate the set of reactor tubes depends on the number of tubes, the outer tube diameter, the tube pitch, and the tube layout (Kakaç and Liu, 2002):

$$Dsi = \left(\sqrt{\frac{4Ntt}{\pi}\frac{\widehat{CL}}{0.93}}\right) Ltp \tag{26}$$

where Ltp is the tube pitch and $\widehat{CL}$ is a geometrical constant that depends on the tube bundle layout (it is equal to 1.0 for a square layout and 0.87 for a triangular layout). Without loss of generality, the value employed for the Ltp corresponds to a pitch ratio (Ltp/dte) equal to 1.25.

The shell and head thicknesses are given by (Fischer et al., 2020):

$$thk_{shell} = \max\left(\frac{\widehat{Pd}(Dsi/2)}{\widehat{S}\widehat{E} - 0.6Pd}, \widehat{thk}_{min}\right) \tag{27}$$

$$thk_{head} = \max\left(\frac{\widehat{Pd}(Dsi/2)}{\widehat{S}\widehat{E} - 0.2Pd}, \widehat{thk}_{min}\right) \tag{28}$$

The maximum pressure difference for the shell and head is the difference between design pressure and atmospheric pressure. The design pressure of the shell is the water vapor pressure (associated with the boiling water temperature) multiplied by a safety factor. The design pressure of the head is the feed inlet pressure also multiplied by a safety factor. The adopted value of the safety factor is 1.1 (Towler and Sinnot, 2007). Finally, the tubesheet thickness is estimated to be 10 % of the shell inner diameter.

The design constraints are the minimum product production, available pressure drop, the length/diameter ratio, and maximum temperature inside the reactor as follows:

$$\widehat{L/D}_{min} \leq L/D \leq \widehat{L/D}_{max} \tag{29}$$

$$F_{product} \geq \widehat{F}^{min}_{product} \tag{30}$$

$$\Delta P \leq \widehat{\Delta Pdisp} \tag{31}$$

$$T^s(z) \leq \widehat{T}_{max} \forall z \tag{32}$$

where $\widehat{F}^{min}_{product}$ is the minimum production of the key product (a minimum conversion could also be used), $\widehat{\Delta Pdisp}$ is the available pressure drop, $\widehat{L/D}_{min}$ and $\widehat{L/D}_{max}$ are, respectively, the minimum and maximum length/diameter ratio and $\widehat{T}_{max}$ is the maximum temperature. The last constraint is important to prevent premature catalyst deactivation. The production ($F_{product}$) and the pressure drop (ΔP) are obtained by integrating the above-presented set of differential equations.

Besides the catalyst bed, the reactor has support balls located at the topside and downside of the bed, and the hold-down support is located only at the bottom. Although there is no reaction in these supporting sections, pressure drop and heat transfer take place. However, these sections are usually considerably smaller than the catalyst bed and are assumed to have negligible effects. The differential equations are solved by integrating the in the range [0, L].

4. Design optimization procedure

The optimization procedure is composed of two steps: Partial Set Trimming followed by Smart Enumeration (Costa and Bagajewicz, 2019). This procedure is suitable for design problems where each solution candidate is defined by a set of values of the design variables presented above, each variable value selected from the list of available discrete options for that variable. Because the design variables presented above are all the independent variables of the problem, once a candidate is selected, the reactor performance can be evaluated and the resulting net present cost can be obtained.

4.1. Set Trimming

Set Trimming is a technique that uses the optimization inequality constraints for eliminating solution candidates as formalized by Costa and Bagajewicz (2019). In Set Trimming, solution candidates are built by considering combinations of discrete values of the design variables. They are gradually eliminated by testing the problem inequality constraints one by one. Therefore, the number of available candidates is gradually reduced. If all constraints are applied to the problem (“Complete Set Trimming”), the set of remaining candidates corresponds to the set of all feasible solutions. Then, the global optimal solution can be identified by a simple sorting procedure based on the calculated objective function.

This procedure was successfully applied for different heat transfer equipment, such as shell-and-tube heat exchangers without phase change (Lemos et al., 2020), kettle vaporizers (Sales et al., 2021), gasketed plate heat exchangers (Nahes et al., 2021) and intensified heat exchangers (Chang et al., 2022). These results show that Set Trimming is a computationally efficient procedure. Set Trimming does not analyze individual candidates employing slow loops, it utilizes computational routines available in different tools to handle large sets of data efficiently (e.g. array operations using NumPy in Python, vectorized operations in Matlab or Scilab, and dynamic sets in GAMS).

However, the application of Set Trimming to the design of fixed-bed reactors cannot involve all the constraints in their original form. The constraints associated with equations (30–32) demand the solution of the set of differential equations of the mathematical model (equations (1–14)), therefore they cannot be applied to an entire set of candidates without a large computational cost. Particularly, the only original constraints that can be used in Set Trimming without having to solve the model for all candidates are the bounds on the length/diameter ratio (equation (29)).

To attain further reductions of the set of candidates using Set Trimming, constraints associated with the numerical solution of the mathematical model can be substituted by a simpler proxy relaxation. Thus, we use relaxations of constraints of equations (30) and (31), where the production constraint is substituted by a catalyst mass constraint, as follows:

$$W^{LB}_{req} \leq W_{cat} \tag{33}$$

$$\Delta P^{LB} \leq \Delta \widehat{Pdisp} \tag{34}$$

where W_{cat} is the catalyst mass, W_{req}^{LB} is the lower bound of the required catalyst mass, and ΔP^{LB} is a lower bound on the pressure drop. The Set Trimming now can be applied as follows: the set of candidates with catalyst mass lower than W_{req}^{LB} is eliminated; something similar takes place for pressure drop, where the set of candidates with pressure drop lower bound larger than $\Delta \widehat{Pdisp}$ is eliminated. A tight relaxation of the reactor temperature constraint (equation (32)) was not identified, therefore there is not a corresponding Proxy Set Trimming associated with this constraint. The details of the construction of the bounds W_{req}^{LB} and ΔP^{LB} are shown below. Because the application of Set Trimming in this problem does not eliminate all of the infeasible candidates, it is called here a "Partial Set Trimming".

Fig. 2 presents the algorithm of the Set Trimming step. The order of the constraints employed in the Set Trimming is: equation (29) → equation (31) → equation (30), where equations (30) and (31) are applied through their proxy representations in equations (33) and (34).

4.2. Smart Enumeration

When Set Trimming is applied using all constraints in their original form, all infeasible candidates are eliminated and a simple sorting procedure after evaluation of the surviving feasible candidates identifies the global optimum. However, if all constraints are not used or if some proxy procedure is used, then not all surviving candidates are feasible. Indeed, Proxy Set Trimming steps let survive a candidate, not because it is feasible, but if it is possibly feasible. Instead of solving the mathematical model of all remaining candidates (i.e. an exhaustive enumeration), we use Smart Enumeration (Costa and Bagajewicz, 2019).

The Smart Enumeration procedure starts by ordering the remaining candidates according to an increasing value of a lower bound of the objective function. The computational cost for the evaluation of this lower bound has to be the lowest possible, without compromising the gap between its value and the rigorous solution too much. Then, the candidates are sequentially evaluated, that is, the full rigorous model of ech candidate is solved following the increasing lower bound order. When a candidate is feasible and has a lower value of the objective function, the incumbent is updated (i.e. it is an upper bound on the optimal solution). The procedure continues until the lower bound of the current candidate becomes larger than the objective function of the incumbent, which guarantees that the global optimum has been found.

In particular, for our reactor design problem, the objective function can be used to arrange the candidates in increasing order at a low computational cost, so a lower bound is not used for this task. Therefore, the evaluation of the mathematical model of the solution candidates following the increasing order of the objective function can be stopped when the first feasible candidate is found.

5. Bounds associated with the proxy set trimming

The lower bound on the required catalyst mass (equation (33)) is obtained by solving the following differential equation:

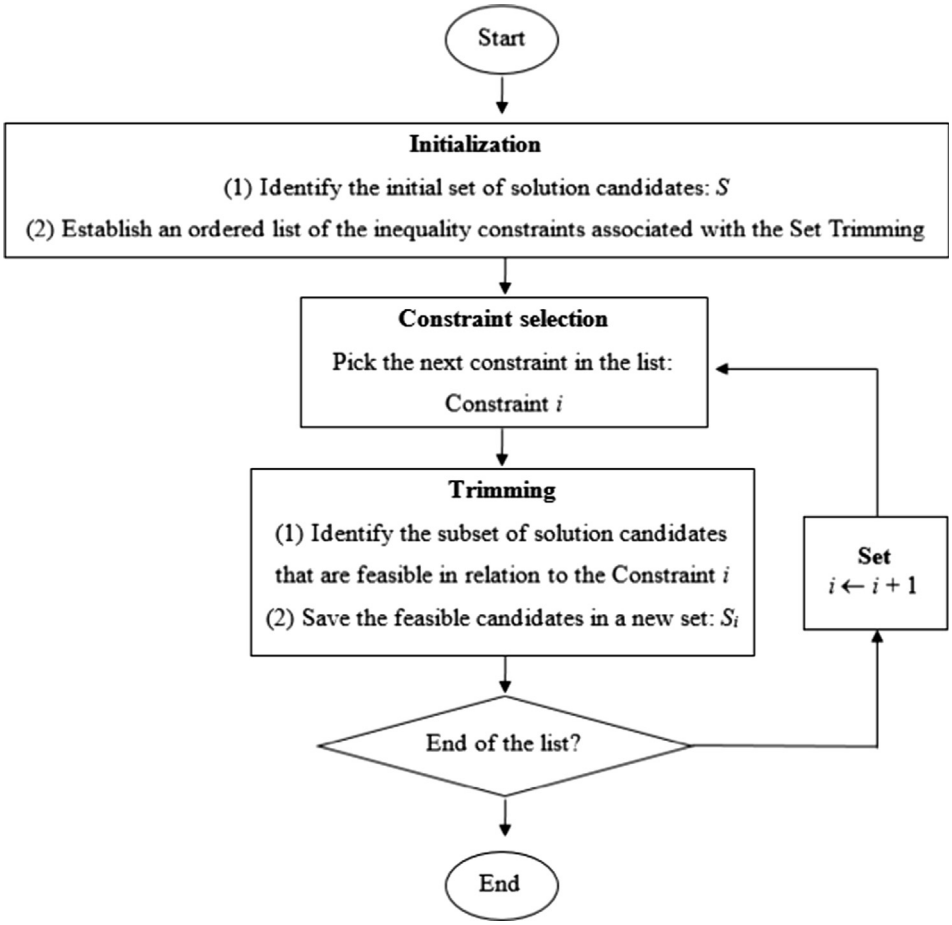

Fig. 2. Set Trimming procedure.

$$\frac{dW_{cat}}{dF_{product}} = \frac{1}{r^{UB}_{product}} \tag{35}$$

The maximum reaction rate ($r^{UB}_{product}$) is calculated with a constant temperature and pressure, using the maximum temperature, $\widehat{T}_{max}$ in equation (32), and the maximum pressure, represented by the inlet value. To guarantee an upper bound, reverse reactions are disregarded. The evaluation of the reaction rate along the numerical integration of equation (35) between the inlet product flow rate and the desired product flow rate is executed considering the corresponding mass balances associated with the stoichiometry of the reaction. Therefore, the Proxy Set Trimming is given by:

$$Ntt\, A_c\, L \rho_B \geq W^{Req}_{cat} \tag{36}$$

In turn, the lower bound on the pressure drop constraint (equation (34)) is given by:

$$\Delta P^{LB} = \left(\frac{\Delta P}{\Delta z}\right)^{LB} L \tag{37}$$

where $\left(\frac{\Delta P}{\Delta z}\right)^{LB}$ is a lower bound of the pressure gradient, evaluated by the RHS of equation (5) considering the following conditions of the gas stream throughout the bed: minimum viscosity and maximum density.

The density and viscosity of the gas phase are dependent on pressure, temperature, and composition. Depending on the specific case, the behavior of these physical properties may be known a priori and the limit condition can be easily selected (e.g. the lowest viscosity value of low-pressure gases corresponds to the lowest temperature). However, if a monotonic behavior cannot be directly established, which is the situation in the present work, it is proposed to solve two small optimization problems before the design optimization to identify the lowest viscosity and the highest density. These extreme values are associated with the lower bound on the pressure gradient, present in Equation (5). The variables of these optimization problems are:

- Temperature: the search space is limited by the minimum temperature (the boiling water temperature or the inlet temperature) and the maximum temperature of the system ($\widehat{T}_{max}$).
- Pressure: the search space is limited by the minimum pressure (inlet gas pressure less the allowable pressure drop) and the maximum pressure of the system (inlet gas pressure).
- Extent of reaction: the extent of reaction expresses the possible gas phase compositions of the reactant mixture and it is limited by the minimum values associated with the production bound.

The sequence of the constraints applied in the Set Trimming is presented in Fig. 3.

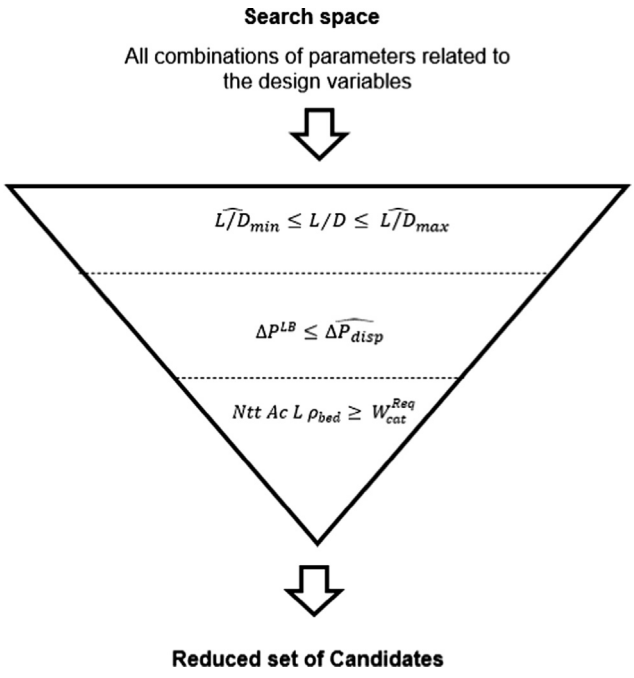

Fig. 3. Set Trimming sequence.

6. Examples

The performance of the proposed design optimization approach is illustrated using two examples involving the synthesis of ammonia and methanol. The quasi-isothermal reactor investigated in this paper is widely used for methanol synthesis (Lurgi reactor) (Moulijn et al., 2013) and its utilization was also investigated for ammonia synthesis (Czuppon, 2001).

The search space of each design problem is presented in Tables 1 and 2. The design problem parameters are presented in Table 3. The data of the catalyst bed of the ammonia and methanol synthesis reactors were originally reported by Palys et al. (2018) and Chen et al. (2011), respectively. The total horizon time of the economic analysis corresponds to 15 years and the interest rate is 10 % for both reactors, associated with a catalyst lifetime of 5 years (Ammoniaknowhow, 2013) for the ammonia synthesis reactor and 3 years for the methanol reactor (therefore, for the ammonia synthesis reactor n_1 = 0, n_2 = 5, n_3 = 10 years and for the methanol synthesis reactor n_1 = 0, n_2 = 3, n_3 = 6, n_4 = 9, and n_5 = 12 years).

The shell, heads, and tubesheet materials are made of carbon steel. The allowable tensile stress, density, and price of carbon steel are, respectively, 127.55 MPa (Engineering Toolbox, 2008), 7840 kg/m^3 (Kloeckner Metals, 2021), and 0.65 US$/kg (Fischer et al., 2020). Due to the hydrogen content in the reactant mixture, the methanol and ammonia reactor tubes are composed of different materials. For the methanol reactor, stainless steel is used, where the allowable tensile stress, density, and price are, respectively, 120.66 MPa (Nickel Institute, 2021), 8000 kg/m^3 (Thyssenkrupp, 2022), and 2.85 US$/kg (Fischer et al., 2020). Finally, the ammonia reactor tubes are composed of 1.25Cr-0.5Mo steel, where the allowable tensile stress, density, and price are, respectively, 103.42 MPa (Metals Pipping, 2016), 7750 kg/m^3 (Piping and Pipeline, 2020) and 2.28 US$/kg (India Mart, 2020). The tube bundle is built in a triangular layout.

The thermal conductivity of the reactant mixture is assumed constant, according to the values obtained from Aspen Plus (0.15 W·m^{-1}K^{-1} and 0.18 W·m^{-1}K^{-1} for the methanol and ammonia synthesis, respectively). In turn, the heat capacity and the density are considered to be a function of temperature, pressure, and composition and were calculated using the Peng-Robison equation of

Table 1
Reactor optimization search space.

Variable	Ammonia synthesis reactor	Methanol synthesis reactor
Total number of tubes, *Ntt*	200, 204, 208, ..., 3000	700, 703, 706, . . ., 3000
Tube alternative (see Table 2)	6, 7, 8, 9, 10	1, 2, 3, 4, 5
Tube length, *L* (m)	3.05, 4.88, 5.49, 6.71, 7.20	1.83, 2.44, 5.49, 6.71, 7.20
Boiling water temperature, *Tc* (K)	600, 610, 620, 630, 640, 645	460, 470, 480, 490, 500, 510, 520

Table 2
Tube alternatives.

Tube alternative	Nominal diameter (in)	Schedule	Inner diameter (m)	Thickness (m)
1	1″	10, 10S	0.0278638	0.0027686
2	1 ¼	10, 10S	0.0366268	0.0027686
3	1 ½"	10, 10S	0.042722800	0.002768600
4	2″	10, 10S	0.0547878	0.0027686
5	2 ½"	10, 10S	0.066929	0.003048
6	1 ¼"	XX	0.0227584	0.009703
7	1 ½"	XX	0.02794	0.01016
8	2″	XX	0.0381762	0.011074
9	2 ½"	XX	0.0449834	0.014021
10	3″	XX	0.05842	0.01524

Table 3
Problem parameters.

Variable	Ammonia synthesis reactor	Methanol synthesis reactor
Bed void fraction, $\widehat{\phi}$	0.400	0.285
Bed density, $\widehat{\rho}_B$ (kg/m^3)	1816.5	851.0
Catalyst diameter, $\widehat{D_p}$ (m)	0.0020	0.0061
Specific surface area, $\widehat{a}_v$ (m^2/m^3)	626.98	626.98
Catalyst price, $\widehat{p}_{cat}$ ($/kg)	15.5	20.6

state for the ammonia synthesis and the Soave-Redlich-Kwong equation of state for the methanol one. Finally, the viscosity is evaluated using the method by Chung et al. (1988).

The proposed approach was implemented in Python with the reactor simulation routine employing the solver LSODA from the SciPy module (Virtanen et al., 2020). Both examples were also addressed using metaheuristic optimization methods, thus providing an assessment of the computational performance of Set Trimming and Smart Enumeration compared with other alternatives from the literature.

6.1. Ammonia synthesis

Ammonia is obtained through the following reaction:

$$N_2 + 3\,H_2 \leftrightarrow 2NH_3 \tag{38}$$

The reaction rate expression used in this article is given by Dyson and Simon (1968):

$$r_{NH_3} = 2k\left[K_a^2 a_{N_2}\left(\frac{a_{H_2}^3}{a_{NH_3}^2}\right)^{0.5} - \left(\frac{a_{NH_3}^2}{a_{H_2}^3}\right)^{0.5}\right] \tag{39}$$

where r_{NH_3} is the rate of formation of ammonia in kmol · m^{-3} · s^{-1} (i.e. this rate is expressed in a volumetric base, it corresponds to the product $\widehat{\rho}_B r_j$ in equations (1), (3), (8), and (9)) and k is given by:

$$k = 2.457 \cdot 10^{11} e^{-\frac{40765}{1.987T}} \tag{40}$$

where T is in Kelvin. The equilibrium constant is given by:

$$\log_{10} Ka = -2.691122\log_{10} T - 5.519265 \cdot 10^{-5} T + 1.848863 \cdot 10^{-5} T^2 + 2001.6 T^{-1} + 2.6899 \tag{41}$$

The effectiveness factor is also taken from Dyson and Simon (1968):

$$\eta = b_0 + b_1 T + b_2 X_{N_2} + b_3 T^2 + b_4 X_{N_2}^2 + b_5 T^3 + b_6 X_{N_2}^3 \tag{42}$$

where X_{N_2} is the nitrogen conversion as measured from the reference mixture which has the following composition: a 3 to 1 H_2 / N_2 ratio and 12.7 % inert, T is in Kelvin and the constants are obtained interpolating the values given in Table 4, according to the system pressure along the bed.

The inlet gas composition is 21.825 % of N_2, 65.475 % of H_2, 5 % of NH_3 and 4 % of both CH_4 and Argon, with 2520 kmol/hr of inlet mole flow rate and 220 bar of pressure.

The tube-side heat transfer coefficient is taken from Leva et al. (1948):

$$\frac{ht\,dti}{k} = 0.813\left(\frac{Dp\,G}{\mu}\right)^{0.9} e^{-\frac{6Dp}{dti}} \tag{43}$$

Because the boiling heat transfer resistance is considerably smaller than the tube-side one, it is considered negligible.

The nonzero binary coefficients of the Peng Robinson equation of state are presented in Table 5 (they were obtained from the Aspen Plus databank).

The bounds associated with the design constraints are:

$$1 \le L/D \le 3 \tag{44}$$

$$F_{product} \ge 5824\text{kg/hr} \tag{45}$$

$$\Delta P \le 3\text{bar} \tag{46}$$

$$T(z) \le 800\,\text{K} \tag{47}$$

6.2. Methanol synthesis

The analysis of the methanol synthesis reactor is based on the kinetic model presented by Vanden Bussche and Froment (1996), which considers two reactions:

$$CO + H_2O \leftrightarrow CO_2 + H_2 \tag{48}$$

$$CO_2 + 3H_2 \leftrightarrow CH_3OH + H_2O \tag{49}$$

These reactions have the following rate expressions in kmol/(kg·s):

Table 4
Ammonia synthesis reactor: Effectiveness factor model parameters.

	Pressure		
Parameter	150 atm	225 atm	300 atm
b_0	−17.539096	−8.2125534	−4.6757259
b_1	0.07697849	0.03774149	0.02354872
b_2	6.900548	6.190112	4.687353
b_3	$-1.082790 \cdot 10^{-4}$	$-5.354571 \cdot 10^{-5}$	$-3.463308 \cdot 10^{-5}$
b_4	−26.424699	−20.86963	11.28031
b_5	$4.927648 \cdot 10^{-8}$	$2.379142 \cdot 10^{-8}$	$1.540881 \cdot 10^{-8}$
b_6	38.93727	27.88403	10.46627

Table 5
Ammonia synthesis reactor: Peng-Robinson nonzero binary coefficients.

Parameter	Value
k_{N_2,H_2}	0.103
k_{N_2,NH_3}	0.2193
k_{N_2,CH_4}	0.0311
$k_{N_2,Ar}$	−0.0026
k_{H_2,CH_4}	0.0156
$k_{NH_3,Ar}$	−0.18
$k_{CH_4,Ar}$	0.023

$$r_{shift} = 10^{-3}\frac{K_1 p_{CO_2}\left[1 - K_3^*\left(\frac{p_{H_2O}p_{CO}}{p_{H_2}p_{CO_2}}\right)\right]}{\left(1 + \left(\frac{K_{H_2O}}{K_8K_9K_{H_2}}\right)\left(\frac{p_{H_2O}}{p_{H_2}}\right) + \sqrt{K_{H_2}p_{H_2}} + K_{H_2O}p_{H_2O}\right)} \quad (50)$$

$$r_{CH_3OH} = 10^{-3}\frac{K_{5_a}K_2K_3K_4K_{H_2}p_{H_2}p_{CO_2}p_{H_2}\left[1 - 1/K^*\left(\frac{p_{H_2O}p_{CH_3OH}}{p^3_{H_2}p_{CO_2}}\right)\right]}{\left(1 + \left(\frac{K_{H_2O}}{K_8K_9K_{H_2}}\right)\left(\frac{p_{H_2O}}{p_{H_2}}\right) + \sqrt{K_{H_2}p_{H_2}} + K_{H_2O}p_{H_2O}\right)^3} \quad (51)$$

where K is the model parameter, K^* and K_3^* are the equilibrium constant of each reaction and p_i is the partial pressure of component i in bar. The values of the kinetic rate parameters are displayed in Table 6.

The equilibrium constants are obtained using the following expressions (Graaf et al., 1986), for T in Kelvin:

$$\log_{10}(K^*) = \frac{3066}{T} - 10.592 \quad (52)$$

$$\log_{10}(K_3^*) = \frac{-2073}{T} + 2.029 \quad (53)$$

The binary coefficients used in the Soave-Redlich-Kwong equation of state are presented in Table 7 (Lovik, 2001).

The design optimization example is based on Chen et al. (2011), which reported reactor and plant data from the methanol synthesis unit of the Tuha Oilfield Company. The feed specifications are given in Table 8, the reactor specifications are presented in Table 9 and the outlet conditions data are depicted in Table 10. The value of the overall heat transfer coefficient reported by Chen et al. (2011) in Table 9 is assumed constant in the reactor design optimization. The reported boiling water temperature is 220 °C.

The objective is to compare the design optimization result proposed in this article with the company reactor. Because the data for the catalyst activity and effectiveness were not provided in Chen et al. (2011), the product of catalyst activity and effectiveness was fitted to minimize the squared relative error between the outlet temperature and methanol production given in Table 10. The obtained value is 0.72.

The bounds associated with the design constraints are:

$$1 \le L/D \le 3 \quad (54)$$

Table 6
Methanol synthesis reactor: Kinetic model parameters.

$k = A\exp\left(BR^{-1}T^{-1}\right)$	A	B
$\sqrt{K_{H_2}}$ (bar$^{-0.5}$)	0.499	17,191
K_{H_2O} (bar^{-1})	$6.62\cdot10^{-11}$	124,119
$K_{H_2O}/(K_8K_9K_{H_2})$	3435.38	0
$K\prime_{5a}K\prime_2K_3K_4K_{H_2}$ (mol · kg^{-1} · s · bar^{-1})	1.07	36,696
$K\prime_1$ (mol · kg^{-1} · s · bar^{-2})	$1.22\cdot10^{10}$	−94765

$$F_{product} \ge 11\,283.1\text{kg/hr} \quad (55)$$

$$\Delta P \le 3\text{bar} \quad (56)$$

$$T(z) \le 290\text{C} \quad (57)$$

The Proxy Set Trimming associated with the required catalyst mass constraint (equation (33)) involves the synthesis reaction depicted in equation (49), eliminating the reverse reaction, as discussed before. Additionally, both carbon oxides in the feed are considered as carbon dioxide, i.e. it is assumed that the conversion of CO to CO_2 in the water gas shift reaction (equation (48)) is instantaneous.

7. Results

The global optimal solutions for the design of the ammonia and methanol reactors attained by Set Trimming followed by Smart Enumeration are presented in Table 11.

It is possible to observe that the optimization procedure found the same solution for the design of the ammonia synthesis reactor using the pseudo-homogeneous and the heterogeneous models. The solutions obtained for the design of the methanol synthesis reactor using different models were slightly different. The optimal design of the methanol synthesis reactor using a heterogeneous model has a cost that is 0.9 % higher than the equivalent result using the pseudo-homogenous model. A more detailed comparison between the solutions is presented later.

The net present cost of the methanol synthesis reactor reported in the literature associated with this example (Chen et al., 2011) is $ 906,431, whereas the proposed design optimization procedure found reactors associated with cost reductions of 4.9 % and 4.0 %, using the pseudo-homogeneous and heterogeneous models, respectively.

Table 12 shows the number of surviving candidates in each trimming and the number of candidates evaluated in the Smart Enumeration, using the pseudo-homogeneous model. The original search space consists of 105,000 and 134,000 candidates and the Set Trimming procedure reduced the list of candidates to 73,722 (29.8 % of the original number) and 59,689, (55.5 % of the original number), for the ammonia and methanol synthesis reactors, respectively. The number of simulations needed to identify the global optimum corresponded to 9.3 % and 9.6 % of the initial search space for the ammonia and methanol reactors, respectively. The corresponding data depicted in Table 12 for the heterogeneous model were the same, except for a slight increase in the number of simulations in the design of the methanol synthesis reactor from 12,943 to 13,252.

Although the required catalyst proxy trimming presents a relevant reduction in the number of candidates in the design of the methanol synthesis reactor, the equivalent trimming in the ammonia synthesis reactor design does not eliminate any candidate, which illustrates the relevance of creating a good constraint approximation. For this constraint, the major problem consists of considering an uniform temperature (the highest possible) for the rate of reaction evaluations, thus rendering a too optimistic scenario, which it was not effective in the ammonia reactor problem.

7.1. Solution comparison between different models

Fig. 4 illustrates the temperature and mole fraction profiles of the optimal solution of the ammonia synthesis reactor obtained using the pseudo-homogeneous and heterogeneous models. It is possible to observe that the profiles are very similar, which

Table 7
Methanol synthesis reactor: Soave-Redlich-Kwong binary coefficients.

k_{ij}	CO_2	CO	H_2	CH_3OH	H_2O	CH_4	N_2
CO_2	0	0	−0.3462	0.0148	0.0737	0.0933	−0.0171
CO	0	0	0.0804	0	0	0.0322	0.013
H_2	−0.3462	0.0804	0	0	0	−0.0222	−0.001
CH_3OH	0.0148	0	0	0	−0.0789	0	−0.214
H_2O	0.0737	0	0	−0.0789	0	0	−0.49
CH_4	0.0933	0.0322	−0.0222	0	0	0	0.031
N_2	−0.0171	0.013	−0.001	−0.214	−0.49	0.031	0

Table 8
Feed specifications of Tuha Oilfield Company methanol reactor.

Parameter	Value
Temperature (°C)	225
Pressure (bar)	69.7
Component flow rate (kg/h)	
CO	10727.9
CO_2	23684.2
H2	9586.5
H_2O	108.8
CH_3OH	770.3*
CH_4	4333.1
N_2	8072.0

* The company reactor feed contains ethanol and methyl formate byproducts, but in this article, they are disregarded and considered as part of the methanol feed.

Table 9
Tuha Oilfield Company methanol reactor and catalyst specifications.

Parameter	Value
Reactor tube diameter	0.04 m
Reactor length	7 m
Number of tubes	1620
Catalyst particle shape	cylinder
Catalyst particle density	1190 kg/m^3
Heat transfer coefficient	118.44 W/(m^2K)

Table 10
Tuha Oilfield Plant data.

	Outlet condition
Temperature (°C)	255
Pressure (bar)	66.9
Mole flow rate (kmol h^{-1})	5592.4
Mass flow rate (kg h^{-1})	57282.8
Volumetric flow (m^3h^{-1})	3780.5
Component flow rates (kg h^{-1})	
CO	4921.0
CO_2	18 316.4
H2	8013.7
H_2O	2309.3
CH_3OH	11 283.1
CH_4	4333.1
N_2	8071.9

explains the reason why the optimization procedure using different models converged to the same reactor.

Fig. 5 presents the temperature and concentration profiles of the gas and solid phases obtained using the heterogeneous model. The small difference between the profiles of each phase indicates that the interfacial transport resistances are not significant. As stated, above, this is the reason why the optimal solution is the same as for the pseudo-homogeneous model.

For the methanol synthesis optimization, the heterogeneous model converged to a reactor with a cost that is slightly higher than the one obtained using the pseudo-homogenous model. Fig. 6 presents the simulation results using both models of the optimal solution obtained using the pseudo-homogenous model. The differences in the profiles are small, but one can observe that there is a slight difference between the methanol mole fraction at the end of the reactor. This difference corresponds to a smaller methanol production predicted by the heterogeneous model (11232.45 kg/hr) compared to the homogenous model (11290.25 kg/hr). However, because the minimum production must be 11283.1 kg/hr (see constraint in equation (55)), the optimal reactor found using the homogeneous model is not feasible according to the heterogeneous model simulation. Consequently, the optimization procedure using the heterogeneous model is forced to identify another candidate with a higher cost, as depicted in Table 11.

The reactor simulation using the heterogeneous model demands a considerably higher computational effort, which affects the optimization. For example, using a computer with a processor i7-8565U 1.8 GHz and 8 GB of RAM memory, the computational times of the optimization using the pseudo-homogenous model are 3017 s and 1735 s for the ammonia and methanol synthesis reactors, respectively. The corresponding computational times of the optimization using the heterogeneous model increase to 144 min and 73 min. This result is expected: the pseudo-homogeneous model requires the integration of a system of ordinary differential equations (ODE), while the heterogenous model requires solving a system of differential–algebraic equations (DAE).

7.2. Comparison with other optimization methods

We compared the performance of Partial Set Trimming followed by Smart Enumeration with GA and PSO for the pseudo-homogenous reactor model. The PSO method was tested using

Table 11
Global optimum solutions of the fixed-bed reactor design.

Design variables	Pseudohomogeneous model		Heterogeneous model	
	Ammonia	Methanol	Ammonia	Methanol
Number of tubes	404	1129	404	1393
Tube alternative	10	4	10	3
Tube length (m)	3.048	5.49	3.048	7.200
Boiling water temperature (K)	645	480	645	490
Objective function ($)	433,284	862,074	433,284	869,848

Table 12
Number of surviving candidates and number of simulations employed in the design using the pseudo-homogeneous model.

		Ammonia	Methanol
Number of surviving candidates	Initial	105,000	134,225
	$L/\widehat{D}_{min} \le L/D \le L/\widehat{D}_{max}$	74,292	73,955
	$\Delta P \le \Delta\widehat{Pdisp}$	73,722	66,066
	$Ntt\pi\frac{Dti^2}{4}L \ge W_{cat}^{req}$	73,722	59,689
Number of evaluations in the Enumeration		9,804	12,943

the routine available in the module PySwarms (Miranda, 2018) using a rounding-off procedure to handle the discrete variables (Sengupta et al., 2018). The GA runs employed the module genetic algorithm (Solgi, 2020) according to Bozorg-Haddad et al. (2017). In all metaheuristic methods, the constraints were handled through the insertion into the objective function of penalty terms:

$$f = fobj + \sum_{i \in violatedconstraint} \left(\widehat{fobj}^{MAX} + 2\widehat{fobj}^{MAX}\Delta g_i\right) \quad (58)$$

where f is the objective function with the penalty term, $fobj$ is the objective function, $\widehat{fobj}^{max}$ is the maximum value of the $fobj$, and Δg_i is the violation of the constraint i. The set of control parameters employed in the GA and PSO algorithms are depicted in Table 13. The control parameters employed in the GA runs correspond to the default values of the genetic algorithm module. The PSO control parameters were the same as those reported in Pedersen (2010).

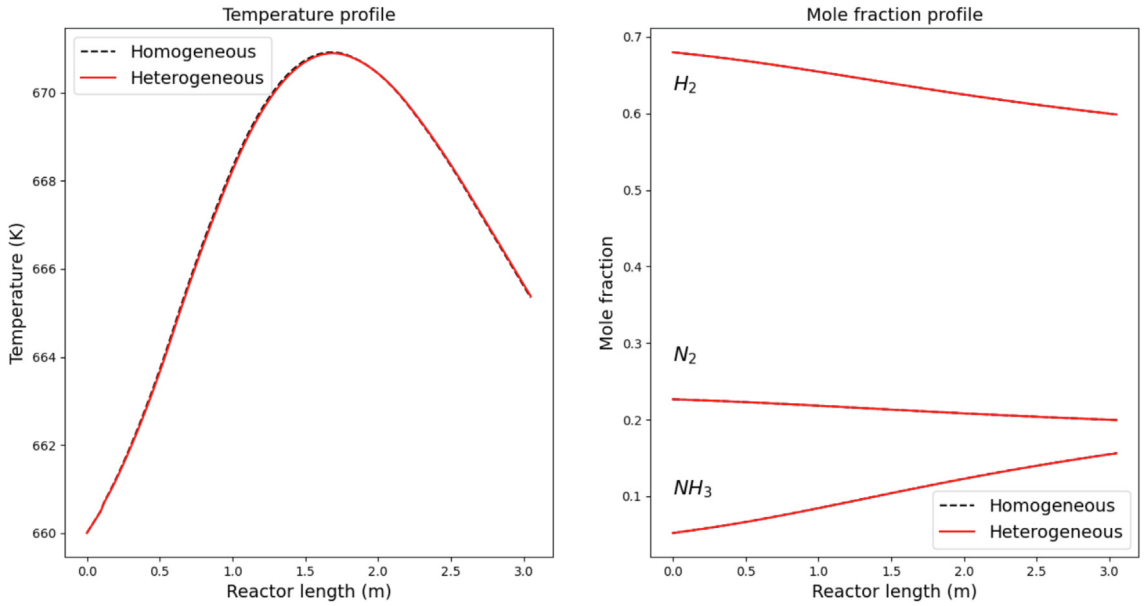

Fig. 4. Temperature and mole fraction profiles of the gas phase of the optimal ammonia synthesis reactor using the pseudo-homogeneous and heterogeneous models.

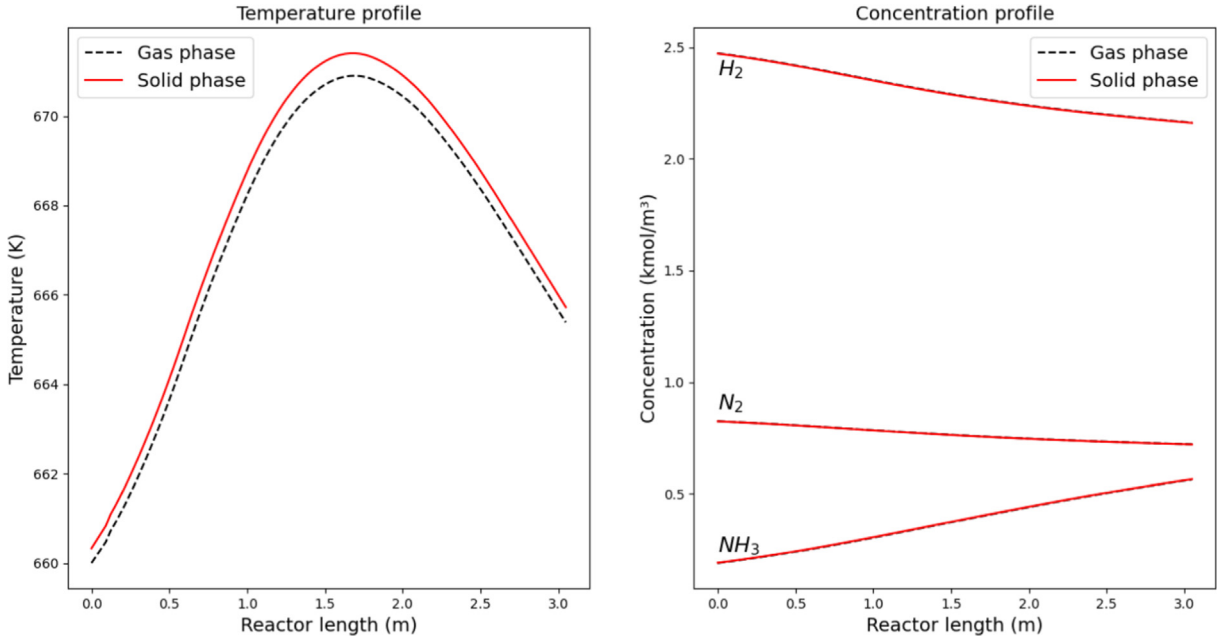

Fig. 5. Temperature and concentration profiles in the gas and solid phases of the optimal ammonia synthesis reactor using the heterogeneous model.

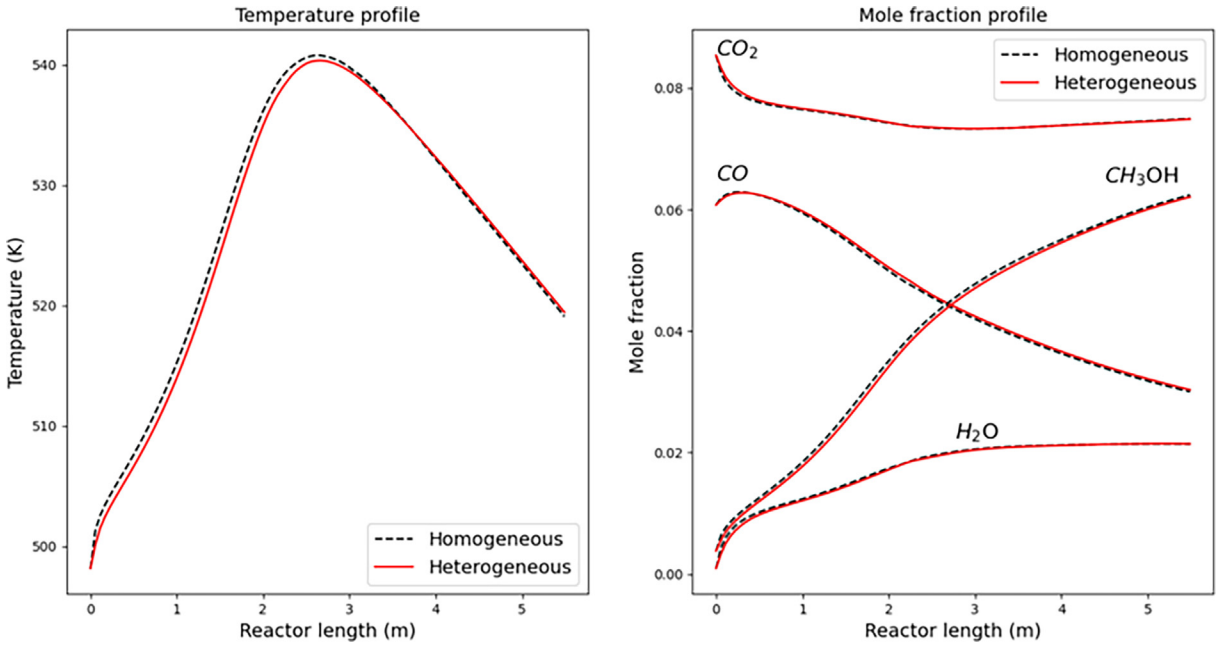

Fig. 6. Temperature and mole fraction profiles of the gas phase of the optimal methanol synthesis reactor using the pseudohomogeneous and heterogeneous models.

Table 13
Set of control parameters employed in the stochastic methods.

Method	Parameter
PSO	Number of particles = 203
	Inertia weight = 0.5069
	Self-confidence factor = 2.5524
	Swarm confidence factor = 1.0056
GA	Population size = 100
	Crossover probability = 0.5
	Mutation probability = 0.1
	Elitism ratio = 0.01
	Parents portion = 0.3
	Crossover type = uniform

Because of the stochastic nature of the metaheuristic methods, the analysis of their performance was based on samples composed of five independent optimization runs. Three different number of iterations were tested for each metaheuristic method. Tables 14 and 15 display the results obtained by each one, compared with the Smart Enumeration. For the metaheuristic methods, we show the best solution, the worst solution, the average value of the objective function of the sample, the fraction of runs where the global optimum was found, and the average elapsed time associated with each method in the sample. The results of the Smart Enumeration in these tables indicate the global optimum and the computational time.

Tables 14 and 15 show that the PSO method present a better performance than the GA method, but both often miss the global optimum. Even considering the highest number of iterations for each test, when the computational times employed by the metaheuristic methods became higher than the Smart Enumeration, the metaheuristic methods may yield solutions with objective function values considerably larger than the global optimum. For example, there are optimal solutions for the ammonia synthesis reactor found by the GA and PSO methods using the maximum number of iterations that are 22.3 % and 12.0 % more expensive than the global optimum.

It is important to observe that the Smart Enumeration procedure does not have any control parameter that must be previously established by the user. Differently, the performance of the metaheuristic methods depends on the tuning of the algorithm control parameters. This aspect can be illustrated in Tables 14 and 15, where the increase of the parameter represented by the maximum number of iterations usually reduces the average value of the objective function in the optimization run samples. However, it is not possible to establish a priori which value must be used. Therefore, it is necessary to apply a tuning procedure, which can be a tedious task. This difficulty is visible just by tuning one parameter. However, the metaheuristic methods have other parameters that are amenable to tuning. Smart Enumeration has no such limitation.

Table 14
Optimization result for the ammonia synthesis fixed-bed reactor design.

Optimal reactor cost (USD)							
Method	GA			PSO			Smart
Number of iterations	50	100	150	20	40	60	
Best	442,205	433,284	455,708	433,284	433,284	433,284	433,284
Average	499,228	503,376	488,126	456,968	454,767	443,677	
Worst	535,793	550,233	530,236	529,280	531,778	485,250	
% Global	0 %	20 %	0 %	60 %	60 %	80 %	
Computing time (s)	1163	2510	4537	1487	3098	4436	3017

Table 15
Optimization result for the methanol synthesis fixed-bed reactor design.

Optimal reactor cost (USD)							
Method	GA			PSO			Smart
Number of iterations	80	160	200	30	60	80	
Best	862,074	862,074	862,074	862,074	862,074	862,074	862,074
Average	874,717	868,681	867,820	865,375	863,840	864,430	
Worst	906,163	879,154	879,023	876,224	867,377	867,377	
% Global	20 %	20 %	20 %	40 %	20 %	40 %	
Computing time (s)	1024	2029	2658	1252	2008	2609	1735

Finally, we point out that optimization runs using smaller increments of the discretization of the boiling water temperature showed no differences in the optimal solution of the ammonia synthesis reactor and a variation of the objective function of the methanol reactor smaller than 0.5 %.

8. Conclusions

In this article, we presented the use of Set Trimming and Proxy Set Trimming followed by Smart enumeration in the design optimization of fixed bed reactors, using two different models. The flexibility of the proposed approach also allows its utilization for the design of other reactor alternatives.

Because the Set Trimming step never eliminates a feasible candidate and the Smart Enumeration always identifies the feasible alternative with minimum cost among the remaining solution candidates, the global optimum solution is guaranteed to be obtained.

A novel aspect included in the Set Trimming in the current paper is the utilization of Proxy Trimming, which is a relaxation of a constraint used to perform the Set Trimming. Not only a simple relaxed expression renders a low computational cost, but, most importantly, it allows a trimming that would not be possible without the relaxation.

Unlike the tedious control parameter tuning associated with metaheuristic algorithms, after the formulation of the problem, it is not necessary to adjust it for different examples (its performance can be different due to the nature of the example, but the structure is always the same).

The performance of this optimization approach was compared with the use of metaheuristics. Differently from the metaheuristic methods, our proposal always obtains the global optimum. Moreover, the numerical results presented above showed several optimization runs using metaheuristic methods with costs considerably higher than the global optimum. This empirical evidence demonstrates that the proposed optimization approach is more robust than metaheuristics, because it never misses the least-cost design.

The proposed approach has also advantages compared with mathematical programming. Mixed-integer nonlinear programming algorithms are prone to convergence problems, but our method is robust in this sense because it does not have convergence iterative loops. Additionally, the utilization of mathematical programming may depend on complex formulations using binary variables to represent the reaction system features. The proposed scheme only depends on the same mathematical model employed for reactor simulation, complemented by approximations for generating the proxy constraints. We also note that our reactor profiles for compositions and temperature are likely to be more accurate than solutions obtained using mathematical programming. Indeed, our technique can use specialized numerical solvers for differential equations (e.g. LSODA), which have smaller truncation errors than the direct utilization of algebraic constraints obtained from the discretization procedures present in mathematical optimization, as employed in Kazi et al. (2021).

Future works may involve the analysis of more complex reaction systems, such as networks of reactors, reactors involving intercooling between multiple beds, quench reactors, etc. Additionally, because this article is focused on the reactor design methodology, new advances can be attained focusing on the extension of the problem to the design of the entire reaction unit, including the identification of the optimal values of the recycle and purge streams and the operating pressure of the system.

CRediT authorship contribution statement

André L.M. Nahes: Methodology, Software, Validation, Investigation, Data curation, Writing – original draft, Writing – review & editing, Visualization. **Miguel J. Bagajewicz:** Conceptualization, Methodology, Investigation, Writing – original draft, Writing – review & editing, Supervision, Project administration. **André L.H. Costa:** Conceptualization, Methodology, Investigation, Writing – original draft, Writing – review & editing, Supervision, Project administration.

Data availability

Data will be made available on request.

Declaration of Competing Interest

The authors declare that they have no known competing financial interests or personal relationships that could have appeared to influence the work reported in this paper.

Acknowledgments

André L.M. Nahes thanks the Coordination for the Improvement of Higher Education Personnel (CAPES) for the scholarships. André L.H. Costa would like to thank the National Council for Scientific and Technological Development (CNPq) for the research productivity fellowship (310390/2019-2) and the Rio de Janeiro State University through the Prociência Program. Miguel Bagajewicz thanks the visiting professor funding from UFRJ for part of the time of the development of this work.

References

AmmoniaKnowHow, 2013. Catalyst deactivation Common causes. Available in: <https://ammoniaknowhow.com/catalyst-deactivation-common-causes/>. Accessed 13 august 2022.

Angira, R., 2011. Simulation and optimization of an auto-thermal ammonia synthesis reactor. Int. J. Chem. React. 9.

Babu, B.V., Angira, R., 2005. Optimal design of an Auto-thermal Ammonia Synthesis Reactor. Comput. Chem. Eng. 29, 1041–1045.

Bozorg-Haddad, O., Solgi, M., Loáciga, H.A., 2017. Meta-heuristic and Evolutionary Algorithms for Engineering Optimization. Wiley, New York.

Carvalho, E.P., Borges, C., Andrade, D., Yuan, J.Y., Ravagnani, M.A.S.S., 2014. Modeling and optimization of an ammonia reactor using a penalty-like method. Appl. Math. Comput. 237, 330–339.

Chang, C., Liao, Z., Costa, A.L.H., Bagajewicz, M.J., 2022. Globally optimal design of intensified shell and tube heat exchangers using complete set trimming. Comput. Chem. Eng. 158, 107644.
Chen, L., Jian, Q., Song, Z., Posarac, D., 2011. Optimization of Methanol Yield from a Lurgi Reactor. Chem. Eng. Technol. 34, 817–822.
Chung, T.H., Ajlan, M., Lee, L.L., Starling, K.E., 1988. Generalized Multiparameter Correlation for Nonpolar and Polar Fluid Transport Properties. Ind. Eng. Chem. Res. 27, 671–679.
Costa, A.L.H., Bagajewicz, M.J., 2019. 110th Anniversary: On the Departure from Heuristics and Simplified Models toward Globally Optimal Design of Process Equipment. Ind. Eng. Chem. Res. 58, 18684–18702.
Cussler, E.L., 1984. Diffusion, Mass Transfer in Fluid Systems. Cambridge University Press.
Czuppon, T.A., 2001. Isothermal Ammonia Converter. U.S Patent No. 6171570 (B1).
Dyson, D.C., Simon, J.M., 1968. Kinetic Expression with Diffusion Correction for Ammonia Synthesis on Industrial Catalyst. Ind. Eng. Chem. Fundamentals. 7, 605–610.
Edgar, T.F., Himmelblau, D.M., Lasdon, L.S., 1989. Optimization of chemical processes. McGraw-Hill Companies.
Engineering ToolBox, 2008. Process Pipes - Allowable Stress vs. Temperature. Available at: <https://www.engineeringtoolbox.com/temperature-allowable-stresses-pipes-d_1338.html> Accessed 13 august 2022.
Ergun, S., 1952. Fluid Flow Through Packed Columns. Chem. Eng. Prog. 6, 89–94.
Fairbanks, D.F., Wilke, C.R., 1950. Difussion Coefficient In Multicomponent Gas Mixtures. Ind. Eng. Chem. Res. 42, 471–475.
Fischer, C.D., Costa, A.L.H., Bagajewicz, M.J., 2020. Nonlinear Model for the Globally Optimal Design of Vertical Vapor Liquid Separation Vessels. Ind. Eng. Chem. Res. 59, 21155–21166.
Froment, G.F., Bischoff, K.B., 1990. Chemical Reactor Analysis and Design. John Wiley & Sons, New York.
Grue, J., Bendtsen, J.D., 2003. Synthesis and Optimisation of a Methanol Process, SIMS 2003 - 44th Conference on Simulation and Modeling on September.
Graaf, G.H., Sijtsema, P.J.J.M., Stamhuis, E.J., Joosten, G.E.H., 1986. Chemical Equilibria in Methanol Synthesis. Chem. Eng. Sci. 41, 2883–2890.
Gut, J.A.W., Pinto, J.M., 2004. Optimal configuration design for plate heat exchangers. Int. J. Heat Mass Transf. 47, 4833–4848.
Hagen, J., 2015. Industrial Catalysis: A Practical Approach. Wiley-VCH Verlag GmbH & Co. KGaA.
Hartig, F., Keil, F.J., 1993. Large-scale spherical fixed bed reactors: Modeling and optimization. Ind. Eng. Chem. Res. 32, 424–437.
India Mart, 2022. Alloy Steel P11 IBR Pipes, Material Grade: ASTM A 335. Available in: <https://www.indiamart.com/proddetail/alloy-steel-p11-ibr-pipes-4076689488.html?fbclid=IwAR2SODh76VJVmZEnt4i6-s2TPvdQSkCGIpSpr6IqV1Lw9nR4Ej3J6bCYfKo>. Accessed 15 july 2022.
Kakaç, S., Liu, H., 2002. Heat Exchangers: Selection, Rating, and Thermal Design. CRC. Press, Boca Ráton.
Kazi, S.R., Short, M., Biegler, L.T., 2021. Heat exchanger network synthesis with detailed exchanger designs: Part 1. A discretized differential algebraic equation model for shell and tube heat exchanger design. AIChE J. 67, e17056.
Kloeckner metals, 2021. What is the density of Stainless Steel. Available in: <https://www.kloecknermetals.com/blog/what-is-the-density-of-stainless-steel/?fbclid=IwAR3R41YdBAOPMKuZHxbf1_Nsr83rqYyE1Ao16J0DC_N_hQ4RyAFzo0yls0k#:~:text=Carbon%20steel's%20density%20is%20about,makes%20its%20density%20vary%20slightly>. Accessed 13 august, 2022.
Lemos, J.C., Costa, A.L.H., Bagajewicz, M.J., 2020. Set trimming procedure for the design optimization of shell and tube heat exchangers. Ind. Eng. Chem. Res. 59, 14048–14054.
Leva, M., Weintraub, M., Grummer, M., Clark, E.L., 1948. Cooling of Gases through Packed Tubes. Ind. Eng. Chem. 40, 747–752.
Lovik, I., 2001. Modelling, estimation and optimization of the methanol synthesis with catalyst deactivation. Norwegian University of Science and Technology. PhD Thesis –.
Matos, B., Carvalho, K.P., Ravagnani, M.A.S.S., 2021. Maximization of the profit and reactant conversion considering partial pressures in an ammonia synthesis reactor using a derivative-free method. Can. J. Chem. Eng. 99, 232–244.
Metals Piping, 2022. Tensile & Yield Strength of ASTM A335 P11 at Elevated Temperatures. Available in: <http://www.metalspiping.com/tensile-and-yield-strength-of-astm-a335-p11-at-elevated-temperatures.html?fbclid=IwAR2vcYjEsClEZ-knprKPV7uS1yraIw2Q3UPQBvMuZVTXq0xYRVz-kz5fS3g#:~:text=Tensile%20%26%20Yield%20Strength%20of%20ASTM%20A335%20P11%20at%20Elevated%20Temperatures,-Home%20%C2%BB%20Technical&text=Designated%20as%20UNS%20K11597%2C%20ASTM,205%20MPa%20at%20room%20temperatures>. Accessed 16 july 2022.
Miranda, L.J., 2018. PySwarms: a research toolkit for Particle Swarm Optimization in Python. J. Open Source Softw.
Moulijn, J.A., Makkee, M., Van Diepen, A.E., 2013. Chemical Process Technology. John Wiley and Sons.
Murase, A., Roberts, H.L., Converse, A.O., 1970. Optimal Thermal Design of an Autothermal Ammonia Synthesis Reactor. Ind. Eng. Chem. Process. Des. Dev. 9, 503–513.
Nahes, A.L.M., Martins, N.R., Bagajewicz, M.J., Costa, A.L.H., 2021. Computational Study of the Use of Set Trimming for the Globally Optimal Design of Gasketed-Plate Heat Exchangers. Ind. Eng. Chem. Res. 60, 1746–1755.
Nickel Institute. Types 304 and 304L Stainless Steels for Low temperature services. Available in: <https://nickelinstitute.org/media/8d91942b4c239eb/ni_inco_328_types304and304lstainlesssteelsforlowtemperatureservice.pdf>. Accessed 13 august 2022.
Palys, M.J., McCormick, A., Cussler, E.L., Daoutidis, P., 2018. Modeling and Optimal Design of Absorbent Enhanced Ammonia Synthesis. Processes. 6, 91.
Pedersen, M.E.H., 2010. Good Parameters for Particle Swarm Optimization. Technical Report no. HL1001.
Piping and Pipeline, 2020. Chemical Composition & Characteristics. Available in: <http://www.pipingpipeline.com/1-25cr-0-5mo-1-25cr-0-5mo-si.html?fbclid=IwAR0FhdTI2hZ94-KRY1GJ0CDB3t8tjMHVQK3vkr0YrmX0iI3rrMAdbHuZINI>. Accessed 15 july 2022.
Reid, R.C., Sherwood, T.K., Prausnitz, J., 1997. The Properties of Gases and Liquids. McGraw-Hill, New York.
Sales, G.M., Queiroz, E.M., Nahes, A.L.M., Bagajewicz, M.J., Costa, A.L.H., 2021. Globally optimal design of kettle vaporizers. Therm. Sci. Eng. Prog. 25, 100962.
Santangelo, D.L.O., Ahón, V.R.R., Costa, A.L.H., 2008. Optimization of Methanol Synthesis Loops with Quench Reactors. Chem. Eng. Technol. 31, 1767–1774.
Sengupta, S., Basak, S., Peters, R.A., 2018. Peters. II Particle Swarm Optimization: A Survey of historical and recent developments with hybridization perspectives. Mach. Learn. Knowl. Extr. 1, 157–191.
Solgi, M., 2020. Genetic algorithm 1.0.1.
Thyssenkrupp, 2022. Density of Stainless Steel. Available in: <https://www.thyssenkrupp-materials.co.uk/density-of-stainless-steel?fbclid=IwAR0CGGB8CJu_VHL4N_NsmHjAJ-dujzG9-wMuFJ-OO1YnWEo-JWnS2miApjQ>. Accessed 15 July 2022.
Smith, J.M., 1980. Chemical Engineering Kinetics. McGraw-Hill, New York.
Torcida, M.F., Curto, D., Martín, M., 2022. Design and optimization of CO2 hydrogenation multibed reactors. Chem. Eng. Res. Des. 181, 89–100.
Towler, G., Sinnot, R., 2007. Chemical engineering design: Principles, Practice and Economics of Plant and Porcess Design. Butterworth-Heinemann.
Upreti, S.R., Deb, K., 1997. Optimal design of an Ammonia Synthesis Reactor Using Genetic Algorithms. Comput. Chem. Eng. 21, 87–92.
Vakili, R., Eslamloueyan, R., 2013. Design and Optimization of a Fixed Bed Reactor for Direct Dimethyl Ether Production from Syngas Using Differential Evolution Algorithm. Int. J. Chem. React. 11, 147–158.
Vanden Bussche, K.M., Froment, G.F., 1996. A Steady-State Kinetic Model for Methanol Synthesis and the Water Gas Shift Reaction on a Commercial Cu/ZnO/Al_2O_3 Catalyst. J. Catal. 161, 1–10.
Virtanen, P., Gommers, R., Oliphant, T.E., Haberland, M., Reddy, T., Cournapeau, D., Burovski, E., Peterson, P., Weckesser, W., Bright, J., Walt, S.J., Brett, M., Wilson, J., Millman, K.J., Mayorov, N., Nelson, A.R.J., Jones, E., Kern, R., Larson, E., Carey, C.J., Polat, I., Feng, Y., Moore, E.W., Vanderplas, J., Laxalde, D., Perktold, J., Cimrman, R., Henriksen, I., Quintero, E.A., Harris, C.R., Archibald, A.M., Ribeiro, A.H., Pedregosa, F., Mulbregt, P.V., Scipy 1.0 Contributors,, 2020. Scipy 1.0: Fundamental Algorithms for Scientific Computing in Python. Nat. Methods 17, 261–272.
Wächter, A., Biegler, L.T., 2006. On the Implementation of a Primal-Dual Interior Point Filter Line Search Algorithm for Large-Scale Nonlinear Programming, Mathematical Programming. Math. Program. 106, 25–57.
Yancy-Caballero, D.M., Biegler, L., Guirardello, R., 2015. Optimization of an Ammonia Synthesis Reactor Using Simultaneous Approach. Chem. Eng. Trans. 43, 1297–1302.
Zhou, W., Manousiouthakis, V.I., 2008. Global Capital/Total Annualized Cost Minimization of Homogeneous and Isothermal Reactor Networks. Ind. Eng. Chem. Res. 47, 3771–3782.